Hydrological Sciences Journal

ISSN: 0262-6667 (Print) 2150-3435 (Online) Journal homepage: http://www.tandfonline.com/loi/thsj20

# On the use of a four-parameter kappa distribution in regional frequency analysis

Thomas Rodding Kjeldsen, Hyunjun Ahn & Ilaria Prosdocimi

**To cite this article:** Thomas Rodding Kjeldsen, Hyunjun Ahn & Ilaria Prosdocimi (2017): On the use of a four-parameter kappa distribution in regional frequency analysis, Hydrological Sciences Journal, DOI: 10.1080/02626667.2017.1335400

**To link to this article:** http://dx.doi.org/10.1080/02626667.2017.1335400



Published online: 12 Jun 2017.

HYDROLOGICAL SCIENCES JOURNAL – JOURNAL DES SCIENCES HYDROLOGIQUES, 2017
https://doi.org/10.1080/02626667.2017.1335400



# On the use of a four-parameter kappa distribution in regional frequency analysis

Thomas Rodding Kjeldsen[a], Hyunjun Ahn[b] and Ilaria Prosdocimi[c]

[a]Department of Architecture and Civil Engineering, University of Bath, Bath, UK; [b]Department of Civil and Environmental Engineering, Yonsei University, Seoul, South Korea; [c]Department of Mathematical Sciences, University of Bath, Bath, UK

**ABSTRACT**

New developments are presented enabling the using a four-parameter kappa distribution with the widely used regional goodness-of-fit methods as part of an index flood regional frequency analysis based on the method of L-moments. The framework was successfully applied to 564 pooling groups and was found to significantly improve the probabilistic description of British flood flow compared to existing procedures. Based on results from an extensive data analysis it is argued that the successful application of the kappa distribution renders the use of the traditional three-parameter distributions such as the generalized extreme value (GEV) and generalized logistic (GLO) distributions obsolete, except for large and relatively dry catchments. The importance of these findings is discussed in terms of the sensitivity of design floods to distribution choice.

**ARTICLE HISTORY**
Received 14 October 2016
Accepted 3 April 2017

**EDITOR**
R. Woods

**ASSOCIATE EDITOR**
A. Viglione

**KEYWORDS**
kappa distribution; regional frequency analysis; L-moments; L-moment diagram; design flood estimation; goodness-of-fit

## Introduction

Regional frequency analysis of extreme events based on the index flood method combined with the method of L-moments for parameter estimation has found widespread use in the hydrology and water resources literature (e.g. Hosking and Wallis 1997, Smithers and Schulze 2001, Salinas *et al.* 2014a). But the use of L-moments has also found application in other practical fields concerned with the risk of extreme events, for example coastal engineering (Hosking 2012), earthquake engineering (Thompson *et al.* 2007), wind speed analysis (Pandey *et al.* 2001), dust storms (Dodangeh *et al.* 2012) and financial returns (Tolikas and Gettinby 2009).

A key aspect in the practical utility of the method of L-moments is the use of L-moment diagrams as a tool for aiding in the identification of a suitable frequency distribution to model the available samples. An L-moment diagram typically plots the sample L-kurtosis ($\tau_4$) against the sample L-skewness ($\tau_3$) values and compares these to equivalent theoretical relationships derived for a range of candidate distributions. The proximity of the sample values (or the mean of the sample values in the case of a regional frequency distribution) to the theoretical lines or points can then be used as a selection criterion for the most appropriate type of distribution. Visual inspection of the proximity between sample values and theoretical lines was adopted by, for example, Vogel *et al.* (1993) in an analysis of regional frequency distributions. Others, including Hosking and Wallis (1993) and Kjeldsen and Prosdocimi (2015), have attempted to derive more formal procedures using Monte Carlo simulation in a hypothesis-testing framework, or, for example Peel *et al.* (2001) and Salinas *et al.* (2014a), using moving averages to judge similarity between samples and theoretical distributions.

For distributions with four parameters or more, the range of possible ($\tau_3$, $\tau_4$) combinations is represented by an area on the L-moment diagram, rather than a line, rendering the traditional graphical goodness-of-fit methods inappropriate. While most regional frequency studies consider mainly two- or three-parameter distributions, Wallis *et al.* (2007) adopted the four-parameter kappa distribution for regional frequency analysis of daily rainfall extremes. The kappa distribution has also been used for extreme value analysis of at-site records of extreme rainfall series (e.g. Parida 1999, Park and Jung 2002) and for analysis of extreme flood flow series (Murshed *et al.* 2014). Consequently, new methodological developments allowing assessment of four-parameter distributions using the method of L-moments would be of significant interest for both applied and theoretical frequency analysis of hydrological extremes.

**CONTACT** Thomas Rodding Kjeldsen t.r.kjeldsen@bath.ac.uk

The aim of this study is to extend the goodness-of-fit (GOF) measures for regional frequency distributions developed by Kjeldsen and Prosdocimi (2015) to enable use of four-parameter distributions in conjunction with the L-moment diagram. The new framework will be used to investigate the potential for adopting a four-parameter kappa distribution for regional modelling of British flood events and assess the impact of changing regional distributions on the resulting design flood estimates.

## The four-parameter kappa distribution

The four-parameter kappa distribution was introduced by Hosking (1994) and has been chosen in this study because: (1) it has an established track record in frequency analysis of extreme hydrological events; (2) analytical expressions of high order L-moment ratios are readily available; and (3) the commonly used generalized logistic (GLO), generalized extreme value (GEV), general Pareto (GPA) and Gumbel models are all special cases of this distribution. Consider $X$ to be a random variable representing the annual maximum events, the cumulative distribution function (cdf) of the kappa distribution is defined as:

$$F(x) = \left\{1 - h[1 - k(x-\xi)/\alpha]^{1/k}\right\}^{1/h} \quad (1)$$

where $\xi$, $\alpha$, $k$ and $h$ are parameters. The associated quantile function is given as:

$$x(F) = \xi + \frac{\alpha}{k}\left\{1 - \left(\frac{1-F^h}{h}\right)^k\right\} \quad (2)$$

The kappa distribution is a generalization of some of the more commonly used three-parameter distributions: for $k \neq 0$, the GPA, GEV and GLO distributions are all special cases for $h = 1$, $h = 0$ and $h = -1$, respectively. The cdf, quantile function and L-moment parameter estimators for the GLO and GEV distributions can be found in Hosking and Wallis (1997).

Using the method of L-moments, the four-parameter model parameters are estimated using the first and second L-moments ($\lambda_1$ and $\lambda_2$), and the third and fourth L-ratios, the L-skewness ($\tau_3$) and the L-kurtosis ($\tau_4$). The formulas relating the distribution parameters and L-moments are given by Hosking and Wallis (1997) as:

$$\lambda_1 = \xi + \alpha(1 - g_1)/k \quad (3)$$

$$\lambda_2 = \alpha(g_1 - g_2)/k \quad (4)$$

$$\tau_3 = (-g_1 + 3g_2 - 2g_3)/(g_1 - g_2) \quad (5)$$

$$\tau_4 = (-g_1 + 6g_2 - 10g_3 + 5g_4)/(g_1 - g_2) \quad (6)$$

where the function $g_r$ is defined as:

$$g_r = \begin{cases} \frac{r\Gamma(1+k)\Gamma(r/h)}{h^{1+k}\Gamma(1+k+r/h)} & h > 0 \\ \frac{r\Gamma(1+k)\Gamma(-k-r/h)}{(-h)^{1+k}\Gamma(1-r/h)} & h < 0 \end{cases} \quad (7)$$

with $\Gamma(\cdot)$ the gamma function. Using the relationships in Equations (5)–(7), it is possible to derive a contour line of the kappa distribution on the L-moment diagram for fixed values of the $h$ parameter. By fixing $h$ and letting $k$ vary freely, the contour lines are comparable to the lines defined the well-known three-parameter distributions (GLO, GEV, GPA) which represent fixed values of $h$. In practice, the contour lines are defined by following the simple steps below:

(1) Fix the value of $h$
(2) Pick a value of $\tau_3$
(3) Find the associated value of $k$ by solving for $k$ in Equation (5) using the Newton-Raphson method
(4) Calculate the associate value of $\tau_4$ for $k$ and $h$ using Equation (6)
(5) Go back to 2 and change the value of $\tau_3$

When a sufficient number of ($\tau_3$, $\tau_4$) pairs have been established (for a fixed value of $h$), the contour line can be plotted on the L-moment diagram as demonstrated on Figure 1 for regions of the diagram often populated by sampling values derived from hydrological series.

Using the procedure above, and for each value of $\tau_3$ in the interval between −1 and 1 (step by 0.05), eighth-order polynomials (Equation (8)) were fitted to the resulting pairs of ($\tau_3$, $\tau_4$) for selected values of the $h$ parameter (see Table 1 for polynomial coefficients $A_p$), which makes for an easy short-cut for plotting selected contour lines.

$$\tau_4 = \sum_{p=0}^{8} A_p \tau_3^p \quad (8)$$

Though, in principle, the contour lines can be produced for any value of $h$ and $k$ obeying the conditions imposed by Hosking (1994).

The contour lines represent the theoretical relationship between the L-skewness and L-kurtosis for the kappa distribution with a fixed $h$ parameter, and are, in principle, similar to the theoretical lines representing three-parameter distributions (GLO, GEV, GPA, PE3)

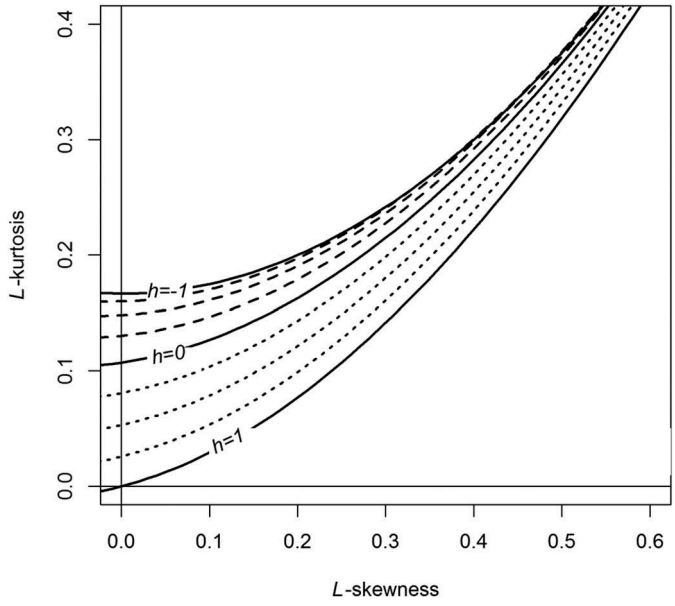


**Figure 1.** L-moment diagram showing contour lines derived for $h = -0.25$, $-0.50$ and $-0.75$ (dashed lines), $h = 0.25$, 0.50, 0.75 (dotted lines) and $h = -1$ (GLO), 0 (GEV), 1 (GPA) (solid lines).

**Table 1.** Polynomial approximations of $\tau_4$ as a function of $\tau_3$ for a kappa distribution with fixed values of the $h$ parameter.

| | $h$ parameter | | | | | | | |
|---|---|---|---|---|---|---|---|---|
| | −1.00* | −0.75 | −0.50 | −0.25 | 0.00† | 0.25 | 0.50 | 0.75 |
| $A_0$ | 0.16667 | 0.15993 | 0.14804 | 0.13031 | 0.10701 | 0.08080 | 0.05313 | 0.02588 |
| $A_1$ | - | 0.02101 | 0.04803 | 0.08044 | 0.11090 | 0.14431 | 0.16889 | 0.18734 |
| $A_2$ | 0.83333 | 0.83146 | 0.82980 | 0.83009 | 0.84838 | 0.86000 | 0.88910 | 0.92319 |
| $A_3$ | - | −0.01700 | −0.03850 | −0.06646 | −0.06669 | −0.12105 | −0.14619 | −0.17023 |
| $A_4$ | - | 0.00635 | 0.01946 | 0.04241 | 0.00567 | 0.05481 | 0.04945 | 0.04428 |
| $A_5$ | - | −0.00151 | 0.00324 | 0.01688 | −0.04208 | 0.00739 | −0.00501 | −0.01053 |
| $A_6$ | - | 0.00071 | −0.01072 | −0.04121 | 0.03763 | −0.02960 | −0.00823 | 0.00197 |
| $A_7$ | - | −0.00248 | −0.01255 | −0.03002 | - | −0.03004 | −0.01744 | −0.00649 |
| $A_8$ | - | 0.00152 | 0.01334 | 0.03802 | - | 0.03380 | 0.01647 | 0.00465 |

*$h = -1$ (GLO) distribution (results from Hosking and Wallis 1997).
†$h = 0$ (GEV) distribution (results from Hosking and Wallis 1997).

as used by Hosking and Wallis (1993) and Kjeldsen and Prosdocimi (2015) in their goodness-of-fit measures. Thus, for a fixed $h$-value the kappa distribution can be included in these tests alongside the commonly used three-parameter distributions.

## An L-moment-based goodness-of-fit measure

The Kjeldsen and Prosdocimi (2015) goodness-of-fit measure uses Monte Carlo simulations to establish the $(1-\alpha)$ x 100% confidence region for the estimated regional average values of $\tau_3$ and $\tau_4$. Assuming the joint distribution of the estimated regional averages of ($\tau_3$, $\tau_4$) is bivariate normal, then the confidence region is represented as an ellipsoid on the L-moment diagram derived using Monte Carlo simulation. It is important to note that the confidence region represented by the ellipsoid is associated with the regional averages and thus exhibits a much smaller variability than the at-site estimates shown in the L-moment diagram. Consequently, the, say, 90% ellipsoid representing the goodness-of-fit measure is not expected to encompass 90% of values from individual sites in the L-moment diagram. Frequency distributions for which the theoretical lines bisect the ellipsoid can thus be considered acceptable as regional frequency models. The final choice of distribution is then based on the minimum value of the Mahalanobis distance, $D$, between the bias corrected regional values of L-skewness and L-kurtosis, $\boldsymbol{t}_B^R$, and points on the different theoretical distribution lines within the confidence region:

$$D^{\mathrm{DIST}} = \left(\boldsymbol{\tau}^{\mathrm{DIST}} - \boldsymbol{t}_B^R\right)^T \boldsymbol{\Omega}^{-1} \left(\boldsymbol{\tau}^{\mathrm{DIST}} - \boldsymbol{t}_B^R\right) \qquad (9)$$

where $\boldsymbol{\Omega}$ is the 2 × 2 covariance matrix of $\boldsymbol{t}_B^R$. Details on the calculations of $\boldsymbol{t}_B^R$ and $\boldsymbol{\Omega}$ using Monte

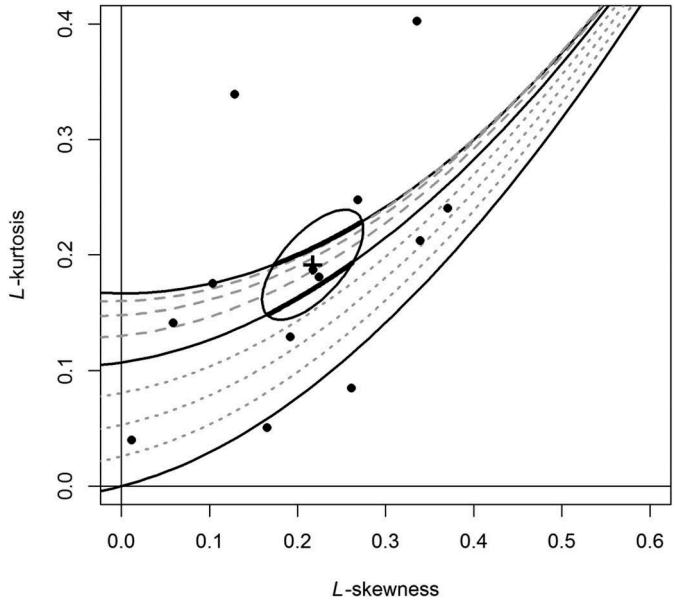


Figure 2. Example of Kjeldsen and Prosdocimi (2015) GOF measure applied with a 90% confidence interval to a pooling group consisting of 13 catchments from the UK (dots). The cross is the regional average L-moment ratio. The thick lines within the ellipsoid highlight that both the GLO and the GEV distribution could be accepted as regional distributions.

Carlo simulations can be found in Kjeldsen and Prosdocimi (2015), and eighth-order polynomials representing the theoretical relationships between $\tau_3$ and $\tau_4$ for a range of three-parameter distributions can be found in Hosking and Wallis (1997, Appendix 12), and for the four-parameter kappa distribution for fixed values of $h$ in Table 1 of this study. An example of the goodness-of-fit measure applied to a pooling group consisting of 13 catchments from the UK is shown in Figure 2.

## Parameter estimation for fixed *h*

Once the $h$ parameter of the kappa distribution is fixed, the remaining location, scale and shape parameters $(\xi, \alpha, \kappa)$ can be estimated using the method of L-moments based on Equations (3)–(5) and (7). First, the fixed value of $h$ is inserted into the expression for $g_r$ in Equation (7). Next, $\tau_3$ in Equation (5) is replaced with the sample value of L-skewness, and the Newton-Raphson method used to find the value of the shape parameter, $\hat{\kappa}$, that solves Equation (5). Next, $\alpha$ and $\xi$ are estimated by replacing $\lambda_1$, $\lambda_2$ and $\kappa$ in Equations (3) and (4) with the corresponding sample values. Finally, the design events, $\hat{x}(F)$, can be calculated using Equation (2) with a fixed value of the $h$ parameter, the non-exceedence probability F, and with the location, scale and shape parameters replaced by their estimated values.

## Case studies

### *Regional flood frequency model in the UK*

In the UK, regional flood frequency analysis is commonly conducted using the pooling group method described in Institute of Hydrology (1999) and later improved by Kjeldsen and Jones (2009). The pooling group method is a combination of the region of influence (ROI) approach (Burn 1990) and the index flood method based on the use of L-moments and annual maximum peak flow data (Hosking and Wallis 1997). Research into the choice of regional frequency distributions for use with the pooling group method by Kjeldsen and Prosdocimi (2015) confirmed previous results reported in the *Flood Estimation Handbook* (Institute of Hydrology 1999) that the three-parameter GLO distribution was most often found to provide the best fit to the data, with the GEV and GNO distributions in second and third place, respectively, and the Pearson Type 3 (PE3) distribution a distant fourth. Prior to the publication of the *Flood Estimation Handbook*, regional flood frequency analysis was based on GEV distributions specified for 10 different geographical regions as described in the *Flood Studies Report* (NERC 1975).

Using a database of annual maximum series from 564 catchments located across the UK, the first four L-moments, $l_1$, $t$, $t_3$ and $t_4$, were estimated for each site. Next, pooling groups were formed for each site based on considerations of hydrological similarity as

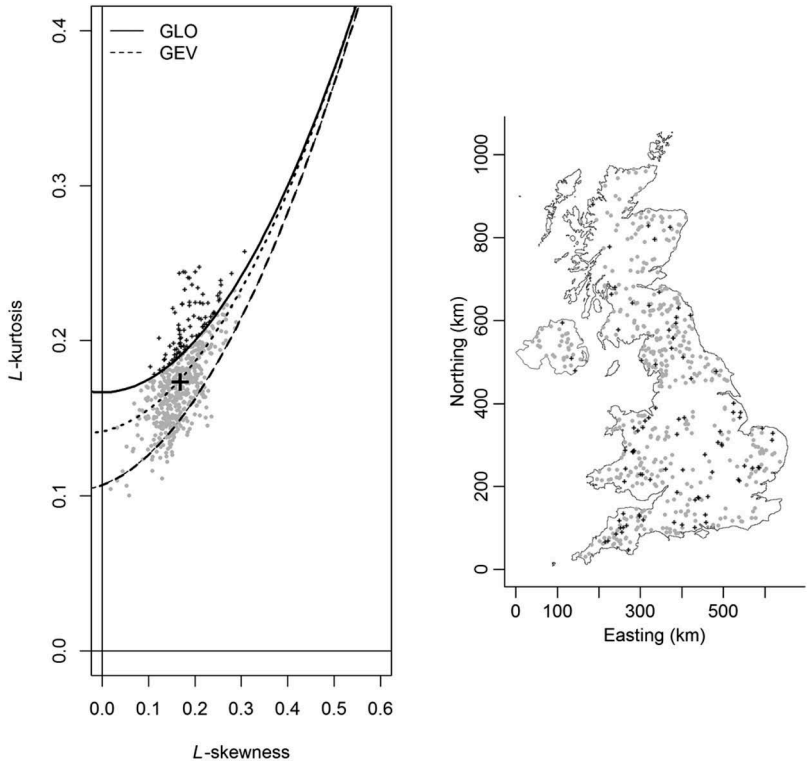


**Figure 3.** (a, left) L-moment diagram showing pooled L-moment ratios for 564 catchment in the UK. Points shown as "+" are located above the GLO line, and therefore not consistent with a kappa distribution. (b, right) Spatial distribution of gauging stations. Gauging stations shown as "+" correspond to catchments with L-moment ratios not consistent with a kappa distribution. The hatched line represent a KAP3 distribution with $h = -0.40$, and the large "+" the national average value of $(\tau_3, \tau_4)$.

described by Kjeldsen and Jones (2009), and the regional (or pooled) L-moment ratios, $t_3^R$ and $t_4^R$, calculated as a weighted average of the individual at-site L-moment ratios contained in the pooling group. Finally, the regional kappa distribution parameters were obtained by using the regional L-moment ratios in combination with Equations (3)–(6) as described by Hosking and Wallis (1997).

Figure 3(a) shows the 564 regional values of L-skewness, $t_3^R$, plotted against the corresponding regional values of L-kurtosis, $t_4^R$, on an L-moment diagram together with the contour line for the KAP3 distribution for $h = -0.40$. Two things are immediately obvious from this figure. First, the majority of data points are located in the area of the L-moment diagram between the theoretical GLO and GEV lines. With reference to Figure 1, this area is characterized by a four-parameter kappa distribution with $h$ in the interval between $h = -1$ (GLO) and $h = 0$ (GEV). It therefore seems reasonable to try to identify a kappa distribution with a fixed (national) value of $h$ as an alternative national flood flow model to replace the current use of the GLO and GEV distributions. Second, a number of data points are located above the GLO distribution (marked with crosses), which suggest that a kappa distribution is not applicable.

Figure 3(b) shows the locations of the 564 gauging stations, again using crosses as in Figure 3(a) to highlight to the stations where the L-moment ratios are located above the GLO line. It is noted that stations with sample L-moments located above the GLO line (crosses) can be found in all regions of the country. No statistically significant relationships were identified between the $h$ parameters and catchment descriptors of the pooling group target sites. This is not surprising as there is already only a weak relationship between L-skewness and catchment descriptors (Kjeldsen and Jones 2009). Thus, for the purpose of this study, a national $h$ parameter value is estimated as a mean value of the $h$ parameter values from each of the 564 pooling groups. Hosking and Wallis (1993) suggested that for cases of L-skewness and L-kurtosis located above the GLO line, the data points are moved down to the GLO line and assigned with an $h$ parameter value of $h = -1$. Making this adjustment, a national average value of $h = -0.40$ was obtained. The contour line of the kappa distribution for a fixed value of $h = -0.40$ is plotted in Figure 3(a) and can be seen to

**Table 2.** Percentages of times a particular distribution is accepted and chosen across the 564 pooling groups. Numbers in parentheses refer to percentages reported by Kjeldsen and Prosdocimi (2015). Note that the three-parameter kappa distribution was not used by Kjeldsen and Prosdocimi (2015).

| | GLO | GEV | GNO | PE3 | KAP3 |
|---|---|---|---|---|---|
| Accepted (%) | 74 | 79 | 71 | 50 | **90** |
| Chosen (%) | 27 (49) | 19 (31) | 8 (12) | 4 (4) | **37** (N/A) |

cut through the centre of the data cloud. Thus, it is reasonable to expect that a kappa distribution with a fixed national $h$ parameter value will provide a better description of the UK flood flow data. Next, this assertion will be tested using the Kjeldsen and Prosdocimi (2015) goodness-of-fit measure combined with the $h = -0.40$ kappa distribution; in the following discussion, this new distribution is denoted KAP3.

For each of the 564 pooling groups, the Kjeldsen and Prosdocimi (2015) goodness-of-fit measure was invoked using the GLO, GEV, GNO, PE3 and KAP3 distributions to assess the fraction of pooling groups that can accept and chose the five candidate distributions. The results are summarized in Table 2 along with the results, in parenthesis, obtained by Kjeldsen and Prosdocimi (2015), who reported a similar analysis on this dataset, but did not include the KAP3 distribution discussed in the present work. The ratio of acceptable distributions remain unchanged, but the number of times each distribution is chosen changes from those reported by Kjeldsen and Prosdocimi (2015) when including the KAP3 distribution.

As can be seen from Table 2, the original results presented in Kjeldsen and Prosdocimi (2015) showed the GLO distribution to give the best fit to the dataset as it was chosen more often (49% of pooling groups). However, introducing the new KAP3 distribution changes the ratio, and KAP3 is more likely to be both accepted (90% compared to 74% for the GLO) and chosen as the regional frequency distribution with 37%, reducing the GLO distribution to only 27%. These results support the use of the new KAP3 model as the default choice for regional frequency estimation in ungauged catchments in the UK, as it is more likely to provide an acceptable representation of the true distribution for the majority of the catchments.

## Climate and scale controls of regional distribution

Investigations of climate and scale controls on the frequency distribution of annual maximum series have been reported in the scientific literature. Analysing at-site annual maximum flood records from Austria, Slovakia and Italy, Salinas *et al.* (2014b) found the GEV distribution to be more appropriate for catchments with medium to high mean annual precipitation, and the GNO distribution more suitable for catchments with low annual average rainfall. These findings were confirmed in a subsequent study of annual maximum series from northern Italy by Persiano *et al.* (2016). Most published studies investigated how catchment properties could give indication of the at-site distribution for a study catchment. Similarly, the potential controls of climate and scale on the choice of the frequency distribution is investigated here, although the focus is now shifted to the regional distribution. Figure 4 shows values of the standard average annual rainfall as measured from 1961 to 1990 (SAAR) against catchment area (natural log scale) for each of the 564 target sites for which pooling groups were formed. Each catchment is classified according to the chosen distribution as per the results in Table 2.

To facilitate the visual comparison, convex hulls were drawn around the cloud of points associated with each of the five distributions (GLO, GEV, GNO, PE3, KAP3). A peeling procedure was applied to the convex hulls (e.g. Hosking 2015) so that they span 90% of the points for each distribution to avoid undue visual distortion by outlying catchments. The plot indicates some degree of scale control on the choice of frequency distribution. In particular, the GLO and KAP3 distributions appear uniquely appropriate for smaller catchments (<50 km$^2$) with high annual rainfall (upper left) while the GEV, GNO and PE3 distributions are more suitable for large catchments (>1000 km$^2$) with relatively modest annual rainfall (lower right). However, for the majority of the catchments of medium size, it is not possible to identify a singular best distribution based on considerations of catchment area or SAAR other than observing that the PE3 distribution appears not to fit data from small and relatively dry catchments (lower left). Plots similar to Figure 3, but with BFIHOST (baseflow index as derived from HOST soils data) and URBEXT (percentage of catchment under urban land cover) substituted for SAAR were also investigated (not shown), but no obvious relationships could be identified. It should be noted that pooling groups might share members with other pooling groups. This is particular true for catchments not well represented in the database of 564 catchments; for example very small catchments. Therefore, the data points in Figure 4 will include aspects of interdependence. However, in real applications, pooling groups would be formed from this dataset, so the conclusions represent the situation faced by hydrologists applying the pooling group method in the UK.

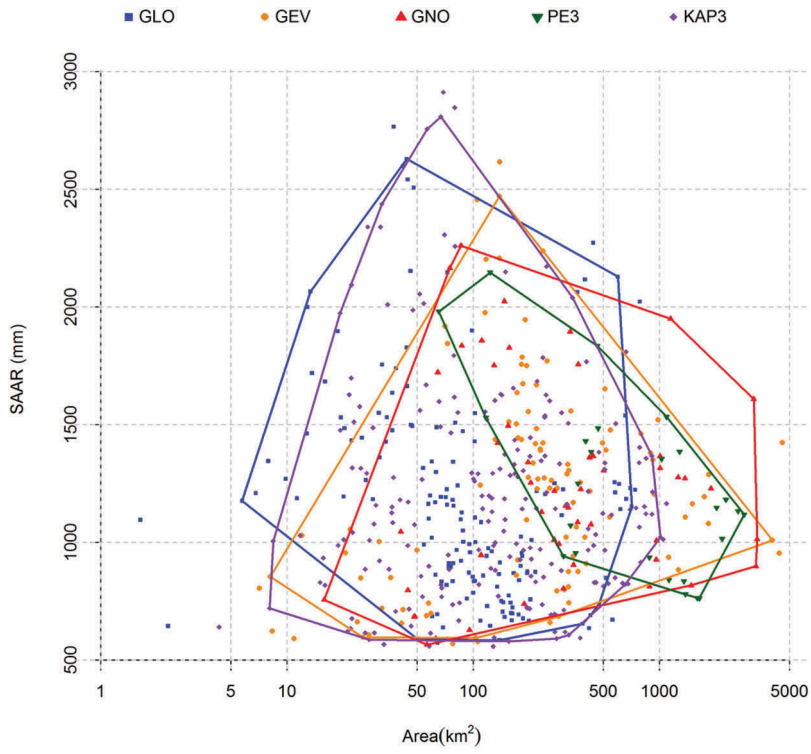


Figure 4. Catchment characteristics of 564 target sites. Symbols and colours refer to the chosen regional frequency distribution for each target catchment. Convex hulls added to aid visual comparison.

## Impact on design flood estimates

Changing the regional distribution from the traditional three-parameter choices: GLO, GEV, GNO or PE3, to the new KAP3 distribution will impact on the resulting flood frequency curves and the magnitude of design flood estimates. The direction and magnitude of this change was assessed by calculating the percentage difference between 100-year events estimated for each of the 564 pooling groups using each of the distributions as:

$$\frac{x_{100}^{\mathrm{KAP3}} - x_{100}^{\mathrm{DIST}}}{x_{100}^{\mathrm{DIST}}} \times 100\%, \quad \mathrm{DIST} = \mathrm{GLO},\ \mathrm{GEV},\ \mathrm{GNO},\ \mathrm{PE3} \tag{10}$$

Thus, positive differences signify that the KAP3 distribution gives higher estimates, and *vice versa*. Next, four subsets of the 564 pooling groups were created corresponding to cases where each of the traditional three-parameter distributions (GLO, GEV, GNO, PE3) were considered acceptable as a regional distribution for the pooling group as per Table 2. Figure 5 shows the percentage differences (Equation (10)) for each of the four subsets plotted against the 100-year event (0.99 quantile) obtained from annual maximum series standardized by their median using the chosen distribution and the standard pooling procedure described in Kjeldsen and Jones (2009). Points plotted using solid dots represent pooling groups where a particular distribution was considered both acceptable and also chosen as the suitable distribution; whereas open symbols represent pooling groups where a distribution was considered acceptable, but not actually chosen as the most suitable distribution based on the Kjeldsen and Prosdocimi (2015) goodness-of-fit measure.

As can be observed from Figure 5, the impact of adopting the KAP3 distribution on the resulting design flood estimates is generally of the order of plus or minus 5%. In comparison with a GLO distribution, the new KAP3 distribution results in lower design flood estimates, typically of the order of 2%. Replacing the GEV, GNO or PE3 distribution with a KAP3 distribution will result in higher design flood estimates. In particular, use of the PE3 distribution can result in differences upwards of 10%, especially for pooling groups with large values of the standardized quantile, i.e. steep growth curves. However, the lack of solid points for large quantiles suggests that, while acceptable, the PE3 distribution is rarely considered to be the optimal distribution for these cases.

## Discussion

The results presented in this study demonstrate that, on a national scale, there is evidence in the observed

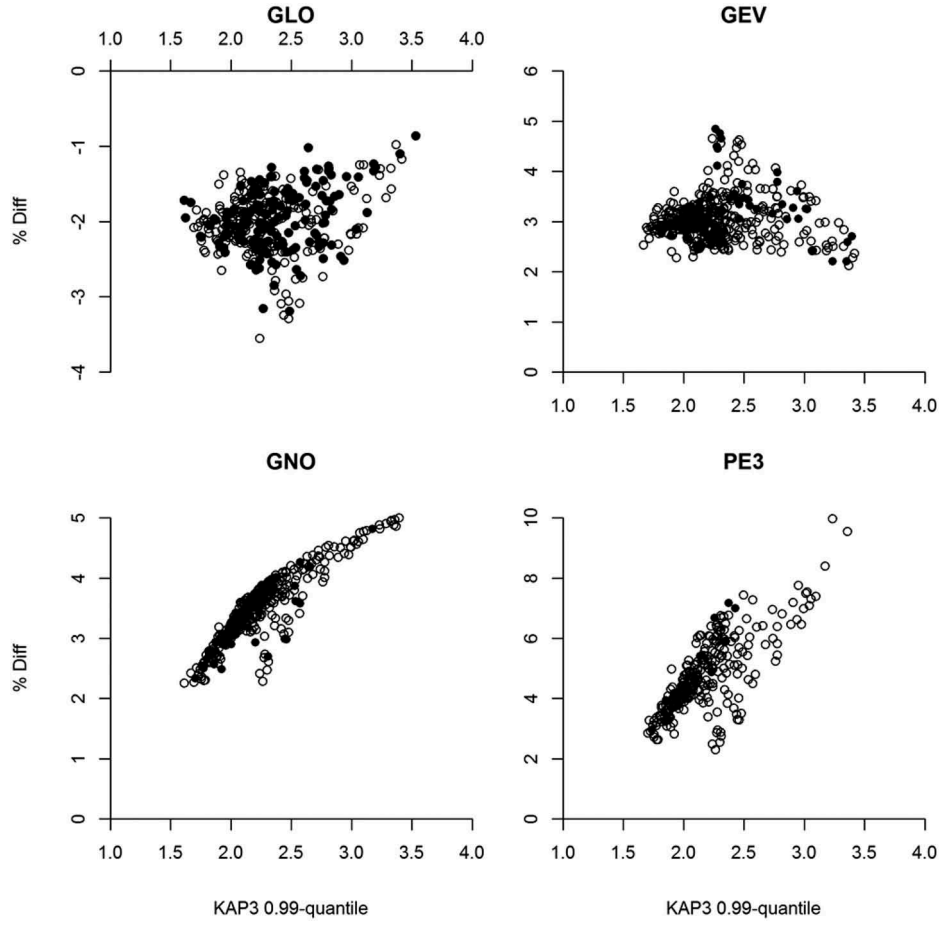


**Figure 5.** Percentage differences between 100-year design event (0.99 quantile) from GLO, GEV, GNO, PE3 distributions and the new KAP3 distribution plotted against the 0.99 quantile derived using KAP3 distribution with standardized AMS. Open circles are used for pooling groups for which either the GLO, GEV, GNO or PE3 were deemed acceptable, and solid circles for pooling groups where the distribution was the best fitting one.

flood flow records that abandoning the traditional choice of a three-parameter distribution such as the GLO or GEV distribution in favour of a four-parameter kappa distribution with fixed $h$ parameter is beneficial. This discovery was first prompted by visual inspection of an L-moment diagram such as that in Figure 3, showing that for the majority of UK pooling groups, the regional average L-skewness and L-kurtosis values fall in the space between the GLO and GEV lines.

Using the goodness-of-fit measure developed by Kjeldsen and Prosdocimi (2015), a national kappa distribution, KAP3, was found to be an acceptable choice of regional frequency distribution for 90% of all pooling groups, which is considered a noteworthy increase from the 74% and 79% achieved by the GLO and GEV distributions, respectively. It is thus argued here that, using a kappa distribution when undertaking a flood frequency analysis at an ungauged site using the pooling group method (by far the most common practical application), the hydrologist is more likely to adopt a representative distribution using KAP3 than would be the case with either the GLO or GEV distributions. However, a subsequent analysis of the scale and climatological controls on choice of regional frequency distribution showed that for large (>1000 km$^2$) catchments with relatively low annual average rainfall, the GEV, GNO or PE3 distributions were typically the preferred options. Finally, it was shown that adopting a kappa distribution with a fixed $h$ parameter resulted in 100-year design flood estimates that were typically 2% lower than corresponding estimates from a GLO distribution (the current recommended distribution in the UK), while the design events were 2–10% larger than estimates obtained from the GEV, GNO and PE3 distributions.

It must be emphasized that this study does not recommend fitting a four-parameter to individual pooling groups by allowing a free $h$ parameter. It is

well-known that increasing the number of model parameters will increase the sampling variability of the design quantile. The additional parameter introduced in the national model in this study constitutes an increase in the number of parameters compared to a GLO or GEV distribution. However, the parameter is estimated as a weighted average across all 564 pooling groups, and thus the sampling variability is expected to be relatively low, even if some sites are represented in several pooling groups and the annual maximum series at different sites are cross-correlated. A more in-depth study of the trade-offs between improved model structure and increased sampling variability is needed to gain further insight into the merits and performance of the proposed national model compared to the current three-parameter models GLO and GEV.

A number of regional values of L-skewness and L-kurtosis were located above the theoretical GLO line, which is outside the region for which the kappa distribution exists. In this study, this problem was solved by moving these sites down to the GLO line and assigning them a parameter value of $h = -1$. Similar adjustments were made by Parida (1999) when modelling extreme rainfall in India using the kappa distribution with the method of L-moments. However, it might be possible to adopt other flexible four-parameter distributions covering a larger region of the L-moment diagram. For example, Hosking (2015) showed that the L-moment ratios of a SU Johnson distribution can be located above the GLO line. It is plausible that the framework developed in this study for the kappa distribution could be extended to include other four- or five-parameter distributions for which theoretical results concerning the higher-order L-moments are available or could be developed. For example, Hosking (1986) discuss the five-parameter Wakeby distribution and Beran *et al.* (1986) provided theoretical results for the probability weighted moments for the two-component extreme value distribution. However, for both distributions numerical solutions must be deployed to use the method of L-moments, which is probably contributing to the relatively rare use of these models in applied frequency analysis.

## Conclusion

The methodological developments and empirical results presented in this study lead to the following conclusions:

- The three-parameter distributions, such as the GLO, GEV and PE3 traditionally used in regional flood frequency analysis, can be replaced by a more flexible four-parameter kappa distribution.
- The new KAP3 distribution was successfully applied to 564 pooling groups from the UK and was found to give a better description of the regional frequency distribution than the traditional choices of either the GLO or GEV distributions.
- Design flood estimates for a 100-year return period in the UK are generally lowered by 2% when using a KAP3 rather than a GLO distribution, but increased by 2–10% when compared to design estimates from GEV, GNO or PE3 distributions.
- The KAP3 distribution appears to be the best choice for small and wet catchments, whereas the GEV, GNO or PE3 might be a better choice in large dry catchments.

The findings could be used to improve the precision of design flood estimation in the UK, but further research is needed to understand the implications of using a national fourth parameter, $h = -0.40$, on the overall reliability of design floods.

## Acknowledgements

The authors are grateful to the National River Flow Archive for making the hydrological datasets available. An R-code implementation of the Kjeldsen and Prosdocimi (2015) goodness-of-fit measure is available via https://github.com/ilapros/GOFmeas.

## Disclosure statement

No potential conflict of interest was reported by the authors.

## References

Beran, M., Hosking, J.R.M., and Arnell, N., 1986. Comment on "Two-component extreme value distribution for flood frequency analysis" by Fabio Rossi, Mauro Florentino, and Pasquale Versace. *Water Resources Research*, 22 (2), 263–266. doi:10.1029/WR022i002p00263

Burn, D.H., 1990. Evaluation of regional flood frequency analysis with a region of influence approach. *Water Resources Research*, 26 (10), 2257–2265. doi:10.1029/WR026i010p02257

Dodangeh, E., Shao, Y., and Daghestani, M., 2012. L-moments and fuzzy cluster analysis of dust storm frequencies in Iran. *Aeolian Research*, 5, 91–99. doi:10.1016/j.aeolia.2011.10.004

Hosking, J.R.M., 1986. *The theory of probability weighted moments*. Research Report RC12210, New York: IBM Research Division, Yorktown Heights.

Hosking, J.R.M., 1994. The four-parameter kappa distribution. *IBM Journal of Research and Development*, 38 (3), 251–258. doi:10.1147/rd.383.0251

Hosking, J.R.M., 2012. Towards statistical modeling of tsunami occurrence with regional frequency analysis. *Journal of Math-For-Industry*, 4, 41–48.

Hosking, J.R.M., 2015. Nonparametric confidence regions for L-moments. *In*: P. Choudhary, C. Nagaraja, H. Ng. (eds) *Ordered data analysis, modeling and health research methods*. Proceedings in Mathematics & Statistics, 149, 39–53. Cham: Springer.

Hosking, J.R.M. and Wallis, J.R., 1993. Some statistics useful in regional frequency analysis. *Water Resources Research*, 29, 271–281. doi:10.1029/92WR01980

Hosking, J.R.M. and Wallis, J.R., 1997. *Regional frequency analysis: an approach based on L-moments*. Cambridge, UK: Cambridge University Press, 240.

Institute of Hydrology, 1999. *Flood estimation handbook*. Vol. 5. Wallingford: Institute of Hydrology.

Kjeldsen, T.R. and Jones, D.A., 2009. A formal statistical model for pooled analysis of extreme floods. *Hydrology Research*, 40 (5), 465–480. doi:10.2166/nh.2009.055

Kjeldsen, T.R. and Prosdocimi, I., 2015. A bivariate extension of the Hosking and Wallis goodness-of-fit measure for regional distributions. *Water Resources Research*, 51 (2), 896–907. doi:10.1002/2014WR015912

Murshed, M.S., Seo, Y.A., and Park, J., 2014. LH-moment estimation of a four-parameter kappa distribution with hydrologic applications. *Stochastic Environmental Research and Risk Assessment*, 28, 253–262. doi:10.1007/s00477-013-0746-6

NERC, 1975. *Flood studies report*. Vol. 5. London: Natural Environment Research Council.

Pandey, M.D., Van Gelder, P.H.A.J.M., and Vrijling, J.K., 2001. The estimation of extreme quantiles of wind velocity using L-moments in the peaks-over-threshold approach. *Structural Safety*, 23 (2), 179–192. doi:10.1016/S0167-4730(01)00012-1

Parida, B.P., 1999. Modelling of Indian summer monsoon rainfall using a four-parameter kappa distribution. *International Journal of Climatology*, 19 (12), 1389–1398. doi:10.1002/(ISSN)1097-0088

Park, J.-S. and Jung, H.-S., 2002. Modelling Korean extreme rainfall using a kappa distribution and maximum likelihood estimate. *Theoretical and Applied Climatology*, 72 (1–2), 55–64. doi:10.1007/s007040200012

Peel, M.C., *et al.*, 2001. The utility of L-moment ratio diagrams for selecting a regional probability distribution. *Hydrological Sciences Journal*, 46 (1), 147–155. doi:10.1080/02626660109492806

Persiano, S., *et al.*, 2016. Climate, orography and scale controls on flood frequency in Triveneto (Italy). *Proceedings of the International Association of Hydrological Sciences*, 373, 95–100. doi:10.5194/piahs-373-95-2016

Salinas, J.L., *et al.*, 2014a. Regional parent flood frequency distributions in Europe – part 1: is the GEV model suitable as a pan-European parent? *Hydrology and Earth System Sciences*, 18, 4381–4389. doi:10.5194/hess-18-4381-2014

Salinas, J.L., *et al.*, 2014b. Regional parent flood frequency distributions in Europe – part 2: climate and scale controls. *Hydrology and Earth System Sciences*, 18 (11), 4391–4401. doi:10.5194/hess-18-4391-2014

Smithers, J.C. and Schulze, R.E., 2001. A methodology for the estimation of short duration design storms in South Africa using a regional approach based on L-moments. *Journal of Hydrology*, 241 (1–2), 42–52. doi:10.1016/S0022-1694(00)00374-7

Thompson, E.M., Baise, L.G., and Vogel, R.M., 2007. A global index earthquake approach to probabilistic assessment of extremes. *Journal of Geophysical Research: Solid Earth*, 112 (B6). doi:10.1029/2006JB004543

Tolikas, K. and Gettinby, G.D., 2009. Modelling the distribution of the extreme share returns in Singapore. *Journal of Empirical Finance*, 16 (2), 254–263. doi:10.1016/j.jempfin.2008.06.006

Vogel, R.M., Thomas, W.O., and McMahon, T.A., 1993. Flood-flow frequency model selection in Southwestern United States. *ASCE Journal of Water Resources Planning and Management Division*, 119 (3), 353–366. doi:10.1061/(ASCE)0733-9496(1993)119:3(353)

Wallis, J.R., *et al.*, 2007. Regional precipitation-frequency analysis and spatial mapping for 24-hour and 2-hour durations for Washington State. *Hydrology and Earth System Sciences Discussions*, 11 (1), 415–442. doi:10.5194/hess-11-415-2007